DESIGN AND PERFORMANCE OF THE LCLS CAVITY BPM SYSTEM*

R. Lill, W. Norum, L. Morrison, N. Sereno, G. Waldschmidt, D. Walters
Advanced Photon Source, Argonne National Laboratory
Argonne, Illinois 60439 USA
S. Smith, T. Straumann
Stanford Linear Accelerator Center, 2527 Sand Hill Road
Menlo Park, CA 94025 USA

Abstract

In this paper we present the design of the beam position monitor (BPM) system for the LCLS undulator, which features a high-resolution X-band cavity BPM. Each BPM has a TM_{010} monopole reference cavity and a TM_{110} dipole cavity designed to operate at a center frequency of 11.384 GHz. The signal processing electronics features a low-noise single-stage three-channel heterodyne receiver that has selectable gain and a phase locking local oscillator. We will discuss the system specifications, design, and prototype test results.

INTRODUCTION

The LCLS FEL will produce x-ray radiation over the 1.5 to 15-Angstrom wavelength range. To produce x-rays in this regime, the electron and photon beams within the 131-m-long undulator must be collinear to less than 10% of the transverse beam size ($\approx$37 μm rms) over a minimum distance that is comparable to the FEL amplitude gain length ($\approx$10 m) in order to achieve saturation [1,2]. To establish and maintain the electron beam trajectory, a high-resolution BPM system has been designed.

The LCLS undulator hall will house 33 undulators [3]. The BPMs will be located in the drift space between each undulator and at the upstream end of the first undulator for a total of 34 BPMs. There are also two BPMs placed in the linac-to-undulator (LTU) transport line. The BPM system must provide stable and repeatable beam position data for both planes on a pulse-to-pulse basis for up to a 120-Hz repetition rate. The BPMs are critical for beam-based alignment and operation of the FEL.

BPM SYSTEM OVERVIEW

The major subsystems for the LCLS undulator BPM system are the cavity BPM, receiver, and data acquisition components shown in Figure 1. The cavity BPM and downconverter will reside in the tunnel and the analog-to-digital converter (ADC) will be located in surface buildings.

*Work supported by U.S. Department of Energy, Office of Science, Office of Basic Energy Sciences, under Contract No. DE-ACOS-06CH11357.

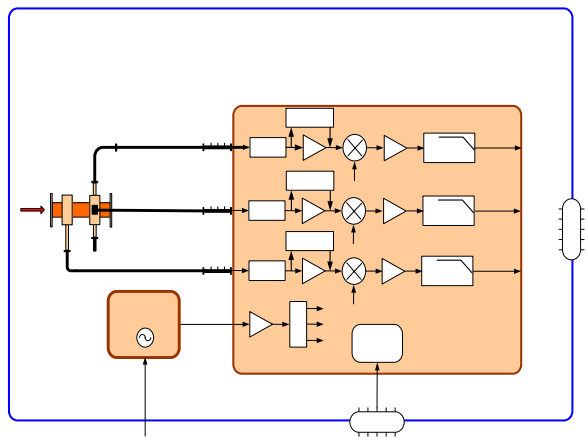

Figure 1: System block diagram.

X-BAND CAVITY DESIGN

The two-cavity BPM design shown in Figure 2 illustrates the cross section of the detector. The beam passes through the monopole reference cavity, shown on the left. The beam excites the TM_{010} monopole mode signal at 11.384 GHz, which is proportional to the beam intensity or charge. The second cavity, 36 mm downstream through the 10-mm-diameter beam pipe, is the TM_{110} dipole cavity shown at the far right. The output of the dipole cavity produces a signal that is dependent on the relative beam displacement r/r_{fix} shown in [4]:

$$V_{out} = \frac{\omega_0}{2}\sqrt{\frac{Z}{Q_{ext}}\left(\frac{R_s}{Q}\right)_{fix}}\,\frac{r}{r_{fix}}q \qquad (1)$$

where R_s/Q is the normalized shunt impedance of the TM_{110} mode, Z is the output line impedance, Q_{ext} is the external quality factor, and q is the charge. The voltage is linearly dependent on the offset and can be scaled.

Horizontal and vertical position signals are generated from the two polarizations of the TM_{110} dipole mode. The polarized fields are coupled to four iris slots equally spaced around the cavity. The magnetic field of the dipole couples to the TM_{110} mode of the rectangular waveguide shown in Figure 2. The distinctive modal patterns of the TM_{010} monopole and TM_{110} dipole modes make it possible to couple only to the dipole mode and reject the monopole mode. This selective coupling technique, pioneered by

Contributed to Particle Accelerator Conference (PAC 2007), 6/25/2007-6/29/2007, Albuquerque, NM, USA

Work supported in part by US Department of Energy contract DE-AC02-76SF00515

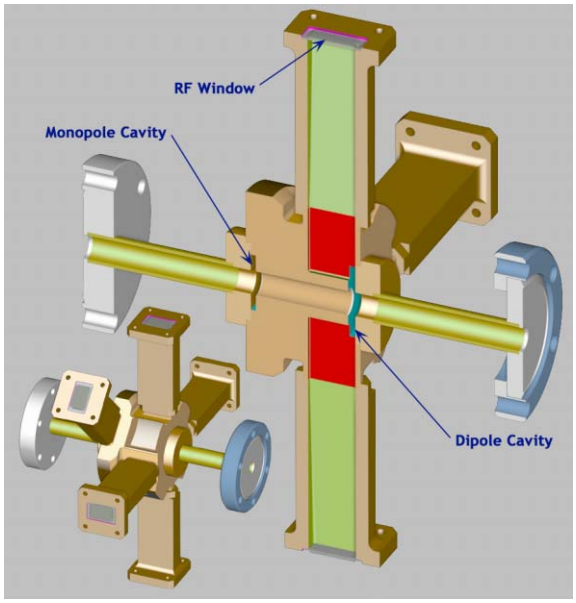

Figure 2: X-band cavity BPM cross section.

SLAC, has been incorporated in this design [5]. The iris couplers are precisely electrical discharge machined (EDMd) into the solid copper block to ensured repeatable and accurate coupling. This technique ensures that the waveguide braze has little or no effect on the cavity performance from the migration of braze material. The dipole cavity was designed as a 4-port device. This is useful for cold testing and also preserves the symmetry. The two unused ports will be terminated with the potential for using them for future diagnostics.

The two cavities are designed to operate at the same frequency and a small amount of tuning is provided for adjustment after brazing. The cavities are pre-tuned before brazing using special fixtures to help maximize machining tolerances. The machining tolerances for the cavity diameters are +0, –15 μm which for the dipole cavity is effectively 367 kHz/μm or 5.5 MHz increase in frequency for the low end tolerance. Tuning pins located on the outer radius of the cavities can be used to increase the resonant frequency. Tuning pins are also located on the end caps, which effectively reduce the resonant frequency when inserted, increasing the cavity wall capacitance and reducing the frequency as $1/\sqrt{LC}$. Tuning pins are also employed on the dipole cavity end cap at 45 degrees to the iris couplers. These pins are used to set the symmetry of the modes and optimize the isolation between planes. Table 1 summarizes the cold test performance for the BPMs that will be used in the 3-BPM test.

Table 1: Cold Test Summary

Serial #	Dipole Freq. (GHz)	Loaded Q	Monopole Freq. (GHz)	Loaded Q
Design Goal	11.384	3550	11.384	3695
R/0	11.384	3310	11.384	3437
001	11.374	3250	11.382	3372
002	11.376	3500	11.383	3436
003	11.377	3371	11.400	3200

RECEIVER DESIGN

The receiver topology used is a single-stage three-channel heterodyne receiver, shown in Figure 1. Each of the three inputs to the receiver is band limited by bandpass filters. The filters provide a 35-MHz bandwidth (-3 dB) centered at 11.384 GHz. The filters also provide a broadband -10 dB return loss match to the cavities. Out-of-band filtering of -60 db reduces unwanted modes from saturating the receiver input. The X-band signals are downconvertered to a 25- to 50-MHz intermediate frequency (IF) in the accelerator tunnel. The signals are first amplified in a low noise amplification (LNA) stage, then translated to a lower IF by mixing with a local oscillator (LO). The LNA is protected against high-power surges by a limiter that is rated at 50 W peak. The dynamic range of the electronics is extended by switching the gain of the receiver. The overall conversion gain/loss is +10 dB in the high gain mode and -15 dB in low gain mode. The LO is a phase-locked dielectric resonant oscillator (PDRO) featuring low phase noise. The LO can be locked to the SLAC 119-MHz timing reference. This has the advantage of synchronizing the data with the beam. The 119 MHz is multiplied by 96 to a LO frequency of 11.424 GHz or four times the LCLS linac frequency. The LO can also run in a free-run mode at 11.424 MHz. The free-run LO frequency is adjustable with a tuning range of 200 MHz centered at 11.424 GHz. A single LO will drive all three channels with an output power +10 dBm. The receiver, LO, bandpass filters, and LO power and distribution board are housed in a 2 in. high × 12 in. wide × 15 in. deep aluminum chassis with integrated heat sink. Special considerations were given to electromagnetic interference (EMI) susceptibility and emissions by using DC blocks on the inputs, EMI gaskets, feed-through pins, and proper grounding. The receiver will be mounted in the tunnel below the undulator girder. The complete receiver unit will not dissipate more that 30 watts. After the X-band signals are downconverted they are conditioned, then cabled out of the tunnel, and sent to the instrumentation rack where the signals are digitized. The SLAC Phase and Amplitude Detector (PAD) will be used for data acquisition. The PAD front end features Linear Technology 130MSPS 16-bit LTC2208 ADCs. The ADCs clocks are synchronized to the 119-MHz timing system in the linac. The raw digital waveform is multiplied point-by-point by a complex $LOe^{j\omega t}$, where ω is the IF frequency. A digital low-pass filter removes the 2ω component leaving a complex baseband signal. A quasi-Gaussian, symmetric, finite-impulse response (FIR) digital filter is chosen to remove the 2ω product as well as out-of-band noise. The complex amplitude of the position signal is normalized by the reference cavity to remove bunch-charge dependence (amplitude) and beam arrival time dependence (phase). Normalized phase and amplitude are converted to position via scaling and rotation by calibration data.

PROTOTYE TESTING

A rigorous test plan has been implemented for the LCLS undulator BPM system. The first phase required the installation of a single-cavity BPM in the injector test stand (ITS) [3]. In this phase the overall design concept was validated. The second phase of testing required the manufacture of three cavity BPMs and supporting electronics. This testing is presently being conducted in the APS LEUTL undulator hall with beam condition similar to the LCLS. The BPMs are mounted on a precision 2-axis translation stage to test and calibrate the BPMs.

Electronic stability tests have been conducted indicating a 100-nm/C drift as shown in Figure 3. The tests were run with system configurations equivalent to those expected in the final installation, including cable lengths. Preliminary data indicates the system performance exceeds the stability requirement < ± 1 μm rms/C for 1 hour and ± 3 μm rms/C for 24 hours.

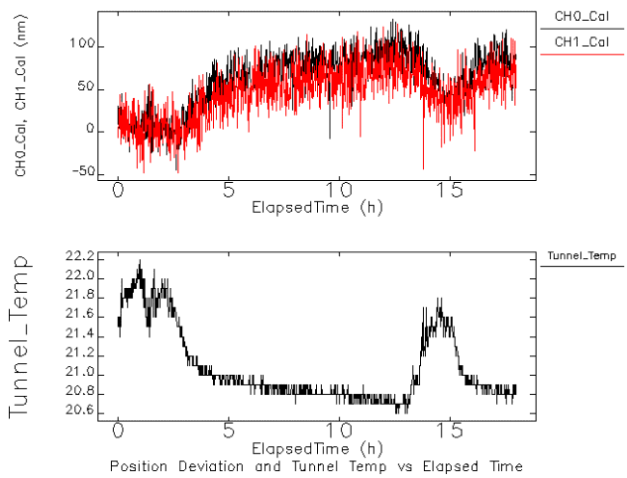

Figure 3: Electronics thermal stability test.

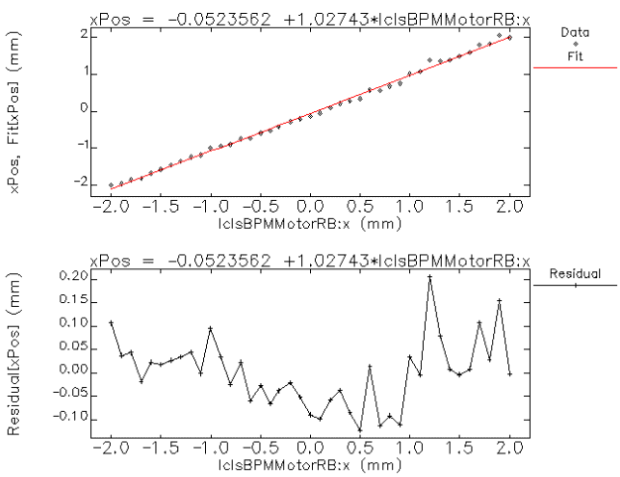

Figure 4: Single BPM test.

CONCLUSIONS

The first test of a single BPM installed in the LEUTL has been conducted. The data shown in Figure 4 illustrate the BPM system range and linearity for a single BPM. These data were taken by moving the translation stage and measuring the beam position, including the beam jitter and electronic noise. The test was conducted with 70-pC charge, which was lower than the 0.2-1.0 nC specified operating range. The addition two BPMs are presently being installed. These BPMs will provide the reference needed to measure single-shot resolution. Preliminary beam tests have produced encouraging results in validating the design for achieving the specified performance.

ACKNOWLEDGMENTS

The authors would like to acknowledge Stephen Milton, Geoff Pile, John Carwardine, Glenn Decker, and Om Singh for many helpful discussions. The authors would also like to thank Randy Zabel and Lester Erwin for all their help with building and testing the prototypes.

REFERENCES

[1] R. Hettel, R. Carr, C. Field, and D. Martin, “Investigation of Beam Alignment Monitor Technologies for the LCLS FEL Undulator,” BIW 98, Stanford CA, May 1998, p. 413.

[2] P. Emma, J. Wu, “Trajectory Stability Modeling and Tolerances in the LCLS,” EPAC 2006, Edinburgh, Scotland, June 2006, http://www.jacow.org.

[3] R. Lill, G. Waldschmidt, D. Walters, L. Morrison, S. Smith, “Linac Coherent Light Source Undulator RF BPM System,” FEL06, Berlin, Germany, July 2006.”

[4] A.Liapine, www.hep.ucl.ac.uk/~liapine/part_one_ waveguides_and_cavities doc.

[5] Z. Li, R. Johnson, S. Smith, T. Naito, J. Rifkin, “Cavity BPM with Dipole-Mode-Selective Coupler,” PAC 03, Portland Oregon, May 2003, http://www.jacow.org.